Talanta 116 (2013) 535–540

Contents lists available at ScienceDirect

Talanta

journal homepage: www.elsevier.com/locate/talanta

Multifunctional inorganic–organic hybrid nanospheres for rapid and selective luminescence detection of TNT in mixed nitroaromatics via magnetic separation

Yingxin Ma, Sheng Huang, Leyu Wang*

State Key Laboratory of Chemical Resource Engineering, School of Science, Beijing University of Chemical Technology, Beijing 100029, China

ARTICLE INFO

Article history:
Received 22 April 2013
Received in revised form
13 July 2013
Accepted 16 July 2013
Available online 20 July 2013

Keywords:
Nanocomposites
TNT detection
Nitroaromatics
Luminescence

ABSTRACT

Rapid, sensitive and selective detection of 2,4,6-trinitrotoluene (TNT) in aqueous solution differentiating from other nitroaromatics and independent of complicated instruments is in high demand for public safety and environmental monitoring. Despite of many methods for TNT detection, it is hard to differentiate TNT from 2,4,6-trinitrophenol (TNP) due to their highly similar structures and properties. In this work, via a simple and versatile method, LaF_3:$Ce^{3+}-Tb^{3+}$and Fe_3O_4 nanoparticle-codoped multifunctional nanospheres were prepared through self-assembly of the building blocks. The luminescence of these nanocomposites was dramatically quenched via adding nitroaromatics into the aqueous solution. After the magnetic separation, however, the interference of other nitroaromatics including 2,4,6-trinitrophenol (TNP), 2,4-dinitrotoluene (DNT), and nitrobenzene (NB) was effectively overcome due to the removal of these coexisting nitroaromatics from the surface of nanocomposites. Due to the formation of $TNT^- - RCONH_3^+$, the TNT was attached to the surface of the nanocomposites and was quantitatively detected by the postexposure luminescence quenching. Meanwhile, the luminescence intensity is negatively proportional to the concentration of TNT in the range of 0.01–5.0 μg/mL with the 3σ limit of detection (LOD) of 10.2 ng/mL. Therefore, the as-developed method provides a novel strategy for rapid and selective detection of TNT in the mixture solution of nitroaromatics by postexposure luminescence quenching.

1. Introduction

Because the nitroaromatic explosives including 2,4,6-Trinitrotoluene (TNT) are highly responsible for environmental pollution, homeland security, and public safety, the rapid, sensitive and selective detection of trace TNT has already attracted wide attention and is gaining increasing concerns [1,2]. Though various strategies have been developed in recent years, lots of versatile and reliable methods for sensitive detection of TNT rely on complicated and expensive instruments including LC–MS, GC–MS, HPLC, surface plasmon resonance (SPR), surface enhanced Raman scattering (SERS) and electrochemical methods [3–9]. Up to now, the sensitive and selective detection of TNT with a portable and simple method, especially capable of differentiating TNT from 2,4,6-trinitrophenol (TNP), is still challenging the analysts [10–13]. Via the color change resulted from the aggregation of gold NPs by the addition of TNT, Mao and coworkers reported a very facile and sensitive method for the colorimetric visualization of TNT [14]. Xia and Zhu developed a fluorescence turn-on sensor for TNT detection via releasing the quantum dots (QDs) from the gold nanorods in the presence of TNT [15]. Base on the stable fluorescence of QDs, Zhang and coworkers have successfully developed many novel strategies for the fluorescence detection of TNT [16–18]. In order to enhance the selectivity of TNT detection, Goldman and coworkers fabricated some QDs-based fluorescence immunoassays for the analysis of TNT [19,20]. Zhang's group also fabricated some molecularly imprinted polymers (MIPs) nanomaterials for TNT selective detection [21–24]. In spite of significant advances have been made in the selectivity and sensitivity of TNT analysis, these analysis schemes can hardly distinguish TNT from TNP in mixed nitroaromatics due to their extremely similar structures and properties. Therefore, highly sensitive, selective, and rapid detection of TNT from the mixture of nitroaromatics in the aqueous solution is still a challenge.

As mentioned above, due to their novel fluorescent properties, QDs have been widely applied for the detection of nitroaromatics [25,26]. Meanwhile, rare earth doped nanomaterials have also drawn wide attentions due to their rich luminescence color, long lifetime, and good photostability [27–35]. To the best of our knowledge, like most of QDs, the excitation of these luminescent

* Corresponging author. Tel./fax: +86 10 6442 7869.
E-mail address: lywang@mail.buct.edu.cn (L. Wang).

0039-9140/$ - see front matter © 2013 Elsevier B.V. All rights reserved.
http://dx.doi.org/10.1016/j.talanta.2013.07.033

materials is often below 400 nm, which is often dramatically absorbed by the nitroaromatics and consequently, the luminescence can be quenched by the nitroaromatics [26,34,36,37]. Therefore, it is difficult to differentiate TNT from other nitroaromatics via luminescence assay based on these luminescent materials, and thus the selective luminescence detection of TNT is hampered. Herein, we fabricated the novel multifunctional nanocomposites by encapsulating the LaF_3:Ce^{3+}–Tb^{3+} luminescent nanoparticles (LNPs) and Fe_3O_4 magnetic nanoparticles (MNPs) in the polymer nanospheres through self-assembly under ultrasonic treatments [38]. Then these amide ($-RCONH_2$) group-enriched inorganic–organic hybrid nanospheres were applied for the selective detection of TNT in the mixture solution of nitroaromatics containing TNT, TNP, DNT, and NB. TNT was absorbed onto the nanospheres via the charge-transfer interaction between amine groups on the nanospheres and the electron-deficient TNT [14,16,18], and then quenched the strong emission of the nanocomposites. As the four kinds of nitroaromatics were added into the nanocomposite colloidal solution, the luminescence was quenched dramatically. After magnetic separation, other three nitroaromatics were removed away from the nanocomposites, and TNT was left on the nanocomposites through the strong charge-transfer interaction of $TNT^- - RCONH_3^+$. The luminescence intensity recovered obviously but still had a certain quenching because of TNT absorption compared with that before the addition of nitroaromatics. Meanwhile, the luminescence intensity decreased step by step with the increase of TNT and is negatively proportional to the TNT concentration. Therefore, multifunctional nanocomposites have been successfully fabricated by a facile and versatile strategy and used for sensitive and selective luminescence detection of TNT in the mixture solution of nitroaromatics with the assistant of magnetic separation.

Via the simple ultrasonication encapsulation strategy, LNPs, MNPs and PSI_{OAm} were successfully fabricated into multifunctional nanocomposites based on self-assembly of the building blocks. Due to the enriched carboxylic groups of PSI_{OAm}, multifunctional nanocomposites are found to be easily dispersed into aqueous media. Under irradiation at 254 nm, the nanocomposites can emit the strong green luminescence centered at 545 nm. As shown in Scheme 1, by adding the mixed nitroaromatics into the solution of nanocomposites, the luminescence of LaF_3 LNPs was dramatically quenched, whereas, it recovered obviously after the removal of 2,4,6-trinitrophenol (TNP), 2,4-Dinitrotoluene (DNT), and nitrobenzene (NB) by magnetic separation. Compared to that of nanocomposites without the addition of nitroaromatics, the luminescence intensity of nanocomposites after magnetic separation still decreased partly because TNT was left on the nanocomposites by charge-transfer interaction between TNT and $RCONH_2$ of PSI_{OAM} matrixes. With the increase of TNT concentration in the mixture solution of nitroaromatics, the luminescence intensity is negatively proportional to the TNT concentration. Therefore, a very simple and highly selective method for the detection of TNT in mixture solution of nitroaromatics was successfully developed based on the postexposure luminescence after magnetic separation.

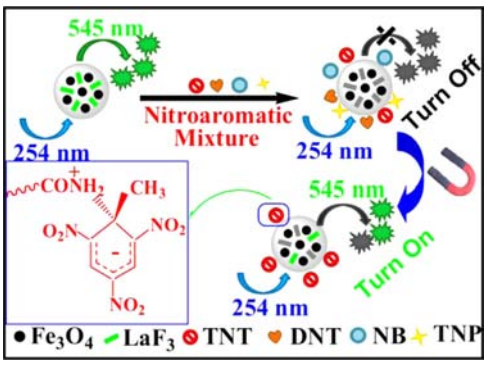

Scheme 1. Schematic diagram for the selective detection of TNT in the mixture solution of nitroaromatics based on the postexposure luminescence quenching of multifunctional nanocomposites after magnetic separation.

2. Experimental section

2.1. Reagents and materials

2,4,6-trinitrotoluene (TNT) and 2,4,6-trinitrophenol (TNP) were supplied by National Security Department of China and recrystallized from ethanol before use. 2,4-dinitrotoluene (DNT) and nitrobenzene (NB) were purchased from Aladdin Chemistry Co. Ltd. (China). These four nitroaromatics were dissolved in the mixed solvent of ethanol and acetonitrile [4:1 (v/v)] to obtain the stock solution before use, respectively. The poly-succinimide (PSI) was supplied from Shijiazhuang Desai Chemical Company. All other reagents were analytical grade and used as received without further purification. Oleic acid was obtained from Alfa. $Fe(NH_4)_2(SO_4)_2 \cdot 6H_2O$ was from Tianjin Fuchen Chemicals Co. (Tianjin, China). $La(NO_3)_3 \cdot 6H_2O$, $Ce(NO_3)_3 \cdot 6H_2O$, and $Tb(NO_3)_3 \cdot 6H_2O$ were purchased from Beijing Ouhe Chemical Company. Ethanol, chloroform, acetonitrile, cyclohexane, NaOH, $NaHCO_3$, Na_2CO_3, NaAc, HAc, Na_2HPO_4, NaH_2PO_4, and NaF were received from Beijing Chemical Company (China).

2.2. Instrument used in synthesis and characterization

The size and morphology of the multifunctional nanocomposites were examined with Supra 55 scanning electron microscope (SEM) (Zeiss, Germany), JEM-1200EX transmission electron microscope (TEM) (JEOL, Japan) and JEM-2100 F high-resolution transmission electron microscope (HRTEM) (JEOL, Japan). Energy dispersive X-ray (EDX) analysis was also recorded on Supra 55 scanning electron microscope (Zeiss, Germany). X-ray diffraction (XRD) patterns were recorded on a Rigaku XRD-A112 X-ray diffractometer which employed Cu Kα radiation of wavelength $\lambda = 1.5418$ Å. The operating current and voltage were kept at 40 mA and 40 kV, respectively. A 2θ range from 10° to 80° was covered in steps of 0.02° with a count time of 2 s. The photoluminescence measurements were carried out on an F-4600 spectrophotometer (Hitachi, Japan). The absorption spectra were conducted on an UNICO 2802PC spectrophotometer with a spectral window range of 190–700 nm. FTIR spectra were performed on Nexus 670 Fourier-transform infrared spectrophotometer (Nicolet, USA). The 50-mL Teflon-lined stainless steel autoclave was used for the synthesis of PSI_{OAM} and nanoparticles.

2.3. Preparation of Fe_3O_4 nanoparticles

Fe_3O_4 magnetic nanoparticles (MNPs) were prepared according to the reported method with some modification [39,40]. In brief, NaOH (1.0 g) was first dissolved in deionized (DI) water (5 mL) followed by the addition of ethanol (15 mL) and oleic acid (10 mL). Finally, 10 mL of aqueous solution containing $Fe(NH_4)_2 \cdot (SO_4)_2 \cdot 6H_2O$ (0.784 g) was added. The mixture was stirred thoroughly and transferred into a Teflon-lined autoclave. Thereafter the autoclave was heated at 180 °C for 10 h and was then allowed to cool naturally to room temperature. The product deposited onto the bottom of the autoclave was collected and washed with cyclohexane and ethanol. The obtained black product was then dispersed in chloroform (4 mL) and stored for later use.

2.4. Synthesis of luminescent $LaF_3:Ce^{3+}-Tb^{3+}$ nanocrystals

Into an autoclave, deionized water (5 mL), ethanol (10 mL) and oleic acid (20 mL) were added. After the mixture was stirred for 10 min at room temperature, 2 mL of the mixed solution (Total $[RE^{3+}]=0.5$ M; RE^{3+} represents the rare earth ions) of $La(NO_3)_3$, $Ce(NO_3)_3$, and $Tb(NO_3)_3$ ($La^{3+}/Ce^{3+}/Tb^{3+}=90/5/5$, solvent: ethanol) was added. Thereafter, 1 mL of aqueous solution of NaF 1 mol L^{-1} was added and the stirring was kept for another 10 min. The autoclave was operated at 180 °C for 16 h. After the autoclave was allowed to cool to room temperature, the white products were collected and washed with cyclohexane and ethanol. This purification cycle was repeated for twice. The final products were dispersed in chloroform (4 mL) and stored for use [40,41].

2.5. Synthesis of PSI_{OAm}

PSI_{OAm} was synthesized according to our previously developed methods with some modification [42,43]. In brief, 1.2 g of polysuccinimide (PSI) [44,45] was dissolved in 24 mL of N, N-Dimethylformamide (DMF) by heating the solution at 60 °C for 10 min, and then 1.22 mL of oleylamine was added. The mixture was heated at 100 °C for 5 h and then automatically cooled to room temperature. Finally, the product (PSI_{OAm}) was collected by precipitating with methanol and centrifuging.

2.6. Synthesis of multifunctional nanocomposites

In a typical procedure, 70 mg of PSI_{OAm} was first dissolved in chloroform (1 mL) followed by the addition of magnetic NPs (MNPs, 5 mg) and luminescent NPs (LNPs, 10 mg). The mixture solution was added to 10 mL of NaOH aqueous solution (0.5 mmol/L) under ultrasonic treatment [38,46–48], and then the brown emulsion was obtained. This emulsion was then stirred at 60 °C for 2 h to remove the chloroform. The multifunctional nanocomposites were collected by centrifugation or magnetic separation, redispersed in deionized water (15 mL) and stored for later use.

2.7. 2,4,6-Trinitrotoluene (TNT) analysis

250 μL of the multifunctional nanocomposite colloidal solution (5 mg/mL) was mixed with various concentration of TNT, and diluted to 1 mL with $NaOH/Na_2CO_3/NaHCO_3$ (0.02 M, pH=12) buffer solution. After magnetic separation, the supernatant was dumped and the nanocomposites were redispersed into the fresh solvents. The luminescence spectra of the mixture solution were measured with excitation wavelength of 254 nm.

3. Results and discussion

The morphology and size distribution of the multifunctional composite nanospheres were observed by transmission electron microscope (TEM). TEM image of the nanocomposites was depicted in Fig. 1a. As can be seen, the nanocomposites whose diameter is 100–250 nm are spherical in shape with smooth surface. The TEM image shows that almost all the composite nanospheres have lots of inorganic nanoparticles in the PSI_{OAm} matrixes and the inorganic nanoparticles have a slightly higher contrast than the PSI_{OAm} matrixes. As shown in Fig. 1b, both the LaF_3 nanorods and Fe_3O_4 nanoparticles were clearly depicted, implying the co-existence of these two kinds of nanocrystals in the PSI_{OAm} matrixes. In addition, the co-existence of LaF_3 nanorods and Fe_3O_4 nanoparticles in the composite nanospheres was further proved by the results of X-ray diffraction (XRD) analysis (Fig. 1c). Fig. 1d shows the strong green photoluminescence of composite nanospheres in the presence of different nitroaromatics before (top line) and after (bottom line) magnetic separation. Under UV light (254 nm), the nanocomposites dispersed in water exhibited strong green luminescence. However, the luminescence was quenched by adding TNT and other nitroaromatics. After magnetic separation, other nitroaromatics were removed away from the nanocomposites but TNT was left via the charge-transfer interaction of $TNT^- - RCONH_3^+$, and the luminescence was turned on again. It is notable that the emission intensity was recovered almost to that of the nanocomposite solution with TNT only. These results suggest that the composite nanospheres have been successfully fabricated and are highly desirable for the selective detection of TNT in the mixture solution of nitroaromatics.

As shown in Fig. 2, before magnetic separation, the luminescence intensity of multifunctional nanocomposites was almost unaffected by pH value both in the absence (Fig. 2a1) and presence of TNT (Fig. 2a2) or the mixed nitroaromatics (Fig. 2a3). Due to the obvious absorption of the UV excitation for LaF_3 by the nitroaromatics including TNT, TNP, NB, and DNT, before the magnetic separation, the luminescence of the nanocomposites was dramatically quenched. After magnetic separation, however, the luminescence of nanocomposites in the absence of TNT was very low under acidic conditions and increased dramatically to the value of the nanocomposites without TNT shown in Fig. 2a1, which can be attributed to the incomplete separation of nanocomposites from the solution before pH 12. In our experiments, only very few nanocomposites were collected from the solution when the pH is less than 7, as a result, the luminescence is very low. At pH 12, the nanocomposites were completely separated via an assistant magnet and thus the luminescence reached the highest value as shown in Fig. 2a1. In the presence of TNT (Fig. 2b2) or the mixed nitroaromatics (Fig. 2b3), the luminescence of the collected nanocomposite colloidal solution increased step by step with the increase of pH value from 4 to 11 after magnetic separation. However, unlike the luminescence of nanocomposites in the absence of nitroaromatics (Fig. 2b1), the luminescence of the nanocomposites in the presence of TNT (Fig. 2b2) or the mixed nitroaromatics (Fig. 2b3) dropped obviously when the pH was increased to 12. As shown in Fig. 2b, the TNT and the mixture of nitroaromatics have the same luminescence quenching ability, which suggests that the TNP, DNT and NB have been removed from the nanocomposites after magnetic separation. In other words, only TNT was attached to the surface through the $TNT^- - RCONH_3^+$ charge-transfer interaction under strong basic conditions (pH=12). As mentioned previously, this $TNT^- - RCONH_3^+$ complex could not form before pH 12. Therefore, the postexposure luminescence detection of TNT was carried out at pH=12.

To investigate the photostability and response speed to the target explosive of the luminescence, the influence of incubation time on the luminescence of nanocomposites in the presence and absence of nitroaromatics was checked. As show in Fig. 3, the luminescence of nanocomposites was stable in the first three hours in the absence of TNT and then quenched instantly by adding TNT (3 μg/mL). Thereafter, the incubation time was prolonged to 6 h, and the luminescence intensity was almost unchanged. After the addition of other three nitroaromatics (TNP/DNT/NB, 1.0/1.0/1.0 μg/mL), however, the luminescence was further quenched dramatically in half minute. The quenched luminescence was kept stable in another three hours and increased as soon as the other three nitroaromatics were removed via magnetic separation. It is notable that the luminescence intensity was recovered nearly to that of nanocomposites in the presence of TNT only. This phenomenon suggests that the multifunctional nanocomposite-based luminescence sensor for TNT detection is rapid, stable, and feasible.

Fig. 4 shows the evolution of luminescence spectra of the multifunctional nanocomposite colloidal solution by increasing

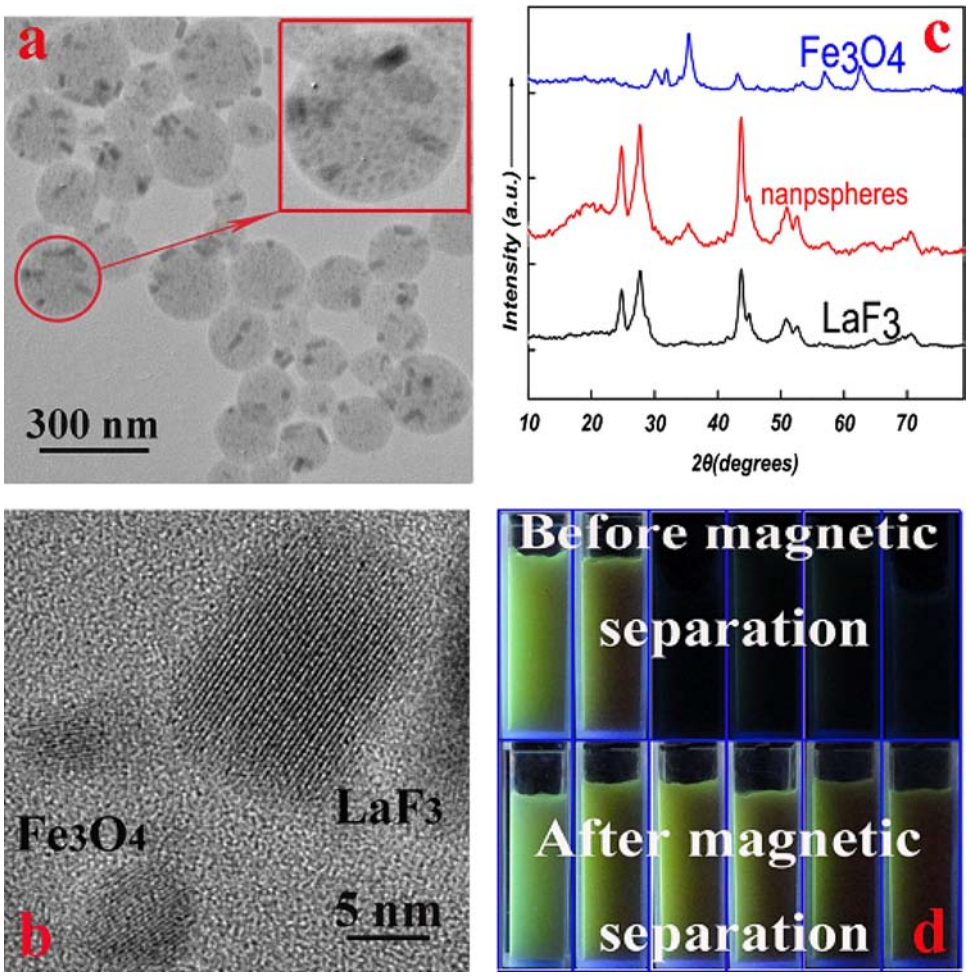

Fig. 1. TEM images of the multifunctional nanocomposites (a), HRTEM image of the nanocomposites (b), XRD patterns of LaF_3 nanocrystals, composite nanospheres, and Fe_3O_4 nanoparticles (c), and luminescence photos of nanocomposite colloidal solution under 254 nm light (from left to right: Blank, in the presence of TNT, TNT–TNP, TNT–DNT, TNT–NB, TNT–TNP–DNT–NB) (d). Concentration of each nitroaromatic is as follows: TNT/TNP/DNT/NB, 3.0/1.0/1.0/1.0 μg/mL.

the TNT concentration. As shown in the spectra, the green luminescence centered at 545 nm decreased step by step with the increase of TNT concentration from 0 to 5.0 μg/mL. Meanwhile, the relative luminescence intensity of the multifunctional nanocomposites is in negative proportion to the concentration of TNT in the range of 0.01–5.0 μg/mL with a 3σ limit of detection (LOD) of 10.2 ng/mL (inset of Fig. 4). The luminescence assay offered a good linearity ($r=0.9981$) with a calibration function of $I=2781.7-123.9C$ ($n=13$) for TNT detection. Herein, the I is the relative luminescence intensity and C is the concentration of TNT (μg/mL). Therefore, the as-prepared nanocomposites can be used for the highly sensitive detection of trace TNT in aqueous solution.

To confirm the highly selective recognition ability of multifunctional nanocomposites for TNT in aqueous media, other three nitroaromatics including DNT, NB, and TNP were mixed with TNT and analyzed with the as-developed method. As shown in Fig. 5, the luminescence of the nanocomposite colloidal solution was quenched while adding 3.0 μg/mL of TNT. However, after the magnetic separation, no luminescence recovery was observed, suggesting the TNT was not removed away from the surface of nanocomposites. Due to the pretty similar chemical structures (Fig. 6) of the nitroaromatics as compared with TNT, the luminescence was further quenched by adding a given concentration of other nitroaromatics. After the treatment of magnetic separation, other three nitroaromatics were removed, but TNT was left on nanocomposites through the interaction between $TNT^- - RCONH_3^+$. As a result, the luminescence intensity of nanocomposites was recovered to that of nanocomposites in the presence of TNT only. Based on this post-exposure luminescence, the as-developed method can be successfully used to for the selective luminescence detection of TNT independent of influence of coexisting TNP, DNT, and NB.

To illustrate the mechanism of the selective luminescence quenching, the UV–visible absorption spectra of TNT, TNP, DNT, and NB (3.0 μg/mL) in the presence of nanocomposites (1.25 mg/mL) dispersed in buffer solution (pH=12; $NaHCO_3-Na_2CO_3-NaOH$, 0.02 M) were carried out, respectively. From Fig. 6, it is clear that all the four kinds of nitroaromatics have a strong absorption band around 250 nm, and the other wide and obvious absorption band at 450 nm was observed from the solution of TNP-nanocomposites. Due to the spectrum overlapping of this absorption and the efficient excitation for LaF_3 NPs (254 nm), all nitroaromatics can quench the luminescence of these as-prepared nanocomposites in aqueous solution. Besides the absorption of the irradiation light (254 nm), the solution of TNT-nanocomposite can also absorb the green (545 nm) emission of LaF_3 NPs, which can be attributed to the formation of an $RCONH_2$-TNT complex whose absorption is located at 545 nm in strong basic solution by the strong charge-transfer interaction [26]. Meanwhile, after magnetic separation, other three nitroaromatics were removed away and only TNT was left by charge-transfer interaction between TNT and nanocomposites. Therefore, the multifunctional nanocomposites can be used for sensitive and selective detection of TNT in mixture solution of nitroaromatics independent of complicated instruments by the postexposure luminescence after magnetic separation.

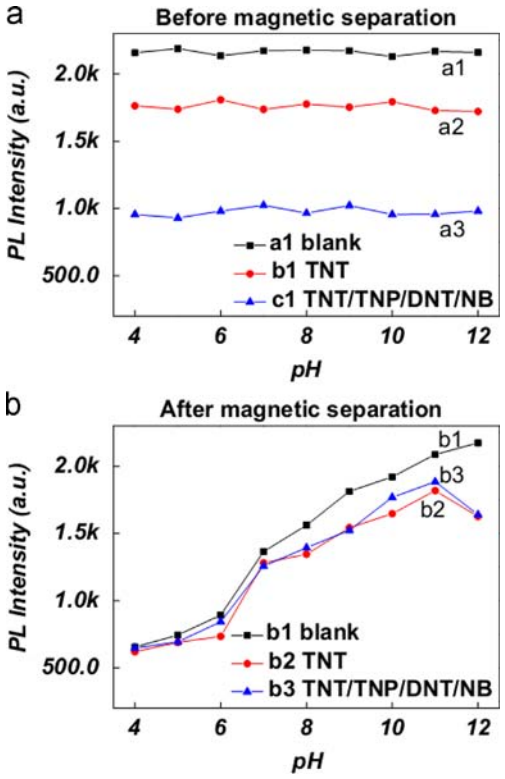

Fig. 2. pH influence on the luminescence intensity of multifunctional nanocomposites (1.25 mg/mL) without (1) and with TNT (2) or the mixed nitroaromatics (3) before (a) and after (b) magnetic separation. Buffer solution and concentration, pH (4–5): $CH_3COOH-CH_3COONa$ (0.02 M); pH (6–8): $NaH_2PO_4-Na_2HPO_4$ (0.02 M); pH (9-12): $NaHCO_3-Na_2CO_3-NaOH$ (0.02 M). Nitroaromatic: (TNT/TNP/DNT/NB, 3.0/1.0/1.0/1.0 μg/mL).

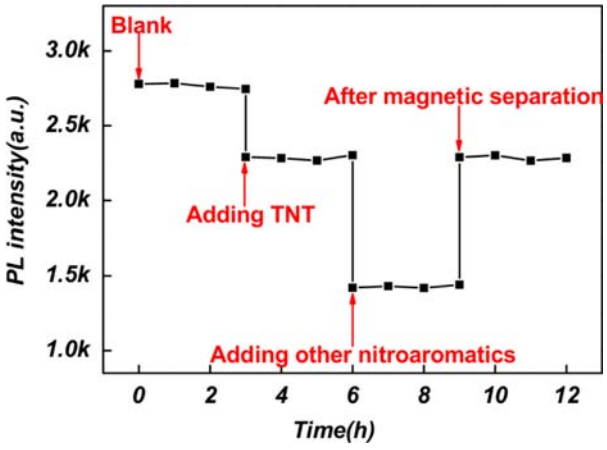

Fig. 3. Effects of incubation time on the luminescence quenching reaction between the nanocomposites (1.25 mg/mL) and nitroaromatics (TNT/TNP/DNT/NB = 3.0/1.0/1.0/1.0 μg/mL) solution at pH = 12.

4. Conclusions

We have developed a novel method to synthesize the multifunctional nanocomposites by encapsulating $LaF_3:Ce^{3+}-Tb^{3+}$ and Fe_3O_4 in PSI_{OAm} polymer matrixes which contains the amide group specially recognizing TNT in the aqueous solution. By adding nitroaromatics into nanocomposites solution, the luminescence intensity was dramatically quenched. However, after magnetic separation, other nitroaromatics were removed away and only TNT was left on the surface of nanocomposites via the $TNT^- - RCONH_3^+$ charge-transfer interaction. As a result, the luminescence was recovered almost to that of the nanocomposites in the presence of TNT only and other nitroaromatics have no effects to the TNT detection. Therefore, a facile and novel nanocomposite-based luminescence assay has been successfully developed for the selective and sensitive detection of TNT in mixture solution of nitroaromatics independent of complicated instruments.

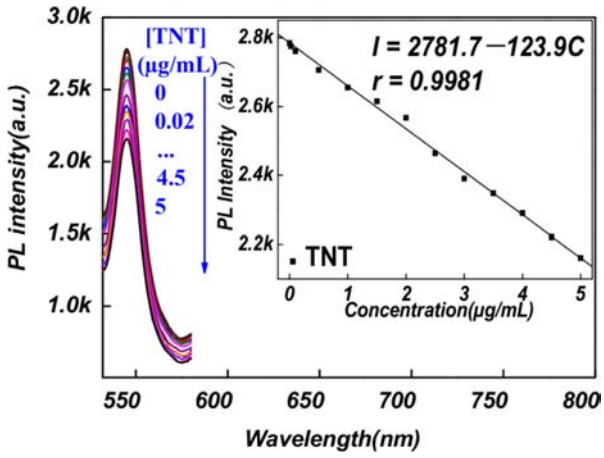

Fig. 4. Luminescence evolution of the multifunctional nanocomposites (1.25 mg/mL) in the presence of various concentration of TNT. Inset: Calibration plot of luminescence intensity versus concentration of TNT. $\lambda_{ex}/\lambda_{em}$ = 254 nm/545 nm.

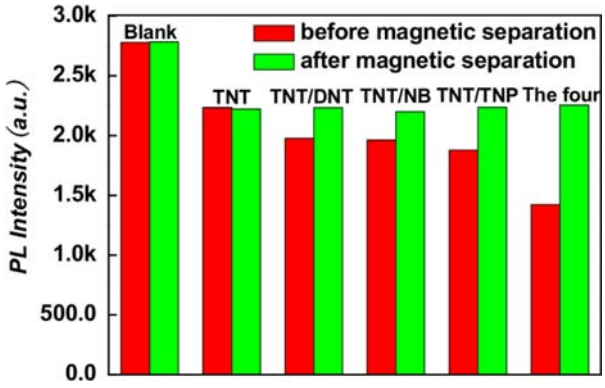

Fig. 5. Luminescence intensity of multifunctional nanocomposites (1.25 mg/mL) in the presence of different nitroaromatics (TNT/TNP/DNT/NB, 3.0/1.0/1.0/1.0 μg/mL) before and after magnetic separation. $\lambda_{ex}/\lambda_{em}$ = 254 nm/545 nm.

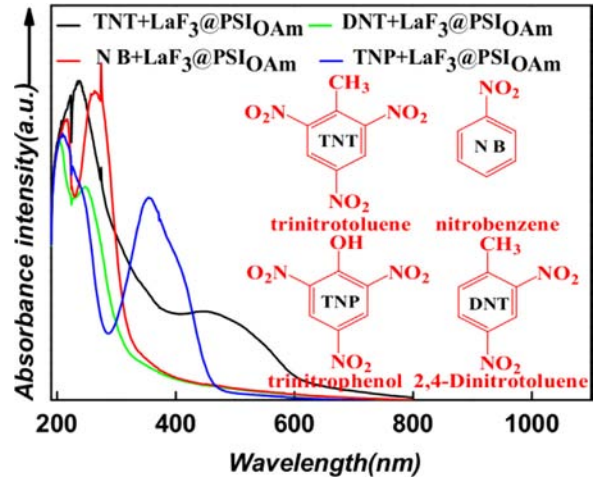

Fig. 6. Absorption spectra of TNT, DNT, NB, and TNP (3.0 μg/mL) in the presence of nanocomposites (1.25 mg/mL). Solvent: buffer solution (pH = 12; $NaHCO_3$–Na_2CO_3–NaOH, 0.02 M). Inset: Chemical structures of the nitroaromatics.

Acknowledgments

This research was supported in part by the National Natural Science Foundation of China (21275015, 21075009), the State Key Project of Fundamental Research of China (2011CB932403 and 2011CBA00503), and the Program for New Century Excellent Talents in University of China (NCET-10–0213), and the Scientific Research Foundation for the Returned Overseas Chinese Scholars, State Education Ministry.

References

[1] T. Alizadeh, M. Zare, M.R. Ganjali, P. Norouzi, B. Tavana, Biosens. Bioelectron. 25 (2010) 1166–1172.
[2] M. Cerruti, J. Jaworski, D. Raorane, C. Zueger, J. Varadarajan, C. Carraro, S.W. Lee, R. Maboudian, A. Majumdar, Anal. Chem. 81 (2009) 4192–4199.
[3] J. Li, C.E. Kendig, E.E. Nesterov, J. Am. Chem. Soc. 129 (2007) 15911–15918.
[4] D.A. Olley, E.J. Wren, G. Vamvounis, M.J. Fernee, X. Wang, P.L. Burn, P. Meredith, P.E. Shaw, Chem. Mater. 23 (2011) 789–794.
[5] K.C. Honeychurch, J.P. Hart, P.R.J. Pritchard, S.J. Hawkins, N.M. Ratcliffe, Biosens. Bioelectron. 19 (2003) 305–312.
[6] G.P. Anderson, S.C. Moreira, P.T. Charles, I.L. Medintz, E.R. Goldman, M. Zeinali, C.R. Taitt, Anal. Chem. 78 (2006) 2279–2285.
[7] R. Batlle, H. Carlsson, P. Tollback, A. Colmsjo, C. Crescenzi, Anal. Chem. 75 (2003) 3137–3144.
[8] M. Berg, J. Bolotin, T.B. Hofstetter, Anal. Chem. 79 (2007) 2386–2393.
[9] I. Cotte-Rodriguez, Z. Takats, N. Talaty, H.W. Chen, R.G. Cooks, Anal. Chem. 77 (2005) 6755–6764.
[10] S.S.R. Dasary, A.K. Singh, D. Senapati, H.T. Yu, P.C. Ray, J. Am. Chem. Soc. 131 (2009) 13806–13812.
[11] Y. Engel, R. Elnathan, A. Pevzner, G. Davidi, E. Flaxer, F. Patolsky, Angew. Chem. Int. Ed. 49 (2010) 6830–6835.
[12] H.R. Nie, Y. Zhao, M. Zhang, Y.G. Ma, M. Baumgarten, K. Mullen, Chem. Commun. 47 (2011) 1234–1236.
[13] R.C. Stringer, S. Gangopadhyay, S.A. Grant, Anal. Chem. 82 (2010) 4015–4019.
[14] Ying Jiang, Hong Zhao, Ningning Zhu, Yuqing Lin, Ping YuLanqun Mao, Angew. Chem. Int. Ed. 47 (2008) 8601–8604.
[15] Y.S. Xia, L. Song, C.Q. Zhu, Anal. Chem. 83 (2011) 1401–1407.
[16] D.M. Gao, Z.Y. Wang, B.H. Liu, L. Ni, M.H. Wu, Z.P. Zhang, Anal. Chem. 80 (2008) 8545–8553.
[17] R.Y. Tu, B.H. Liu, Z.Y. Wang, D.M. Gao, F. Wang, Q.L. Fang, Z.P. Zhang, Anal. Chem. 80 (2008) 3458–3465.
[18] K. Zhang, H.B. Zhou, Q.S. Mei, S.H. Wang, G.J. Guan, R.Y. Liu, J. Zhang, Z.P. Zhang, J. Am. Chem. Soc. 133 (2011) 8424–8427.
[19] E.R. Goldman, I.L. Medintz, J.L. Whitley, A. Hayhurst, A.R. Clapp, H.T. Uyeda, J.R. Deschamps, M.E. Lassman, H. Mattoussi, J. Am. Chem. Soc. 127 (2005) 6744–6751.
[20] I.L. Medintz, E.R. Goldman, M.E. Lassman, A. Hayhurst, A.W. Kusterbeck, J.R. Deschamps, Anal. Chem. 77 (2005) 365–372.
[21] C.G. Xie, B.H. Liu, Z.Y. Wang, D.M. Gao, G.J. Guan, Z.P. Zhang, Anal. Chem. 80 (2008) 437–443.
[22] H.B. Zhou, Z.P. Zhang, C.L. Jiang, G.J. Guan, K. Zhang, Q.S. Mei, R.Y. Liu, S. H. Wang, Anal. Chem. 83 (2011) 6913–6917.
[23] C.G. Xie, Z.P. Zhang, D.P. Wang, G.J. Guan, D.M. Gao, J.H. Liu, Anal. Chem. 78 (2006) 8339–8346.
[24] D.M. Gao, Z.P. Zhang, M.H. Wu, C.G. Xie, G.J. Guan, D.P. Wang, J. Am. Chem. Soc. 129 (2007) 7859–7866.
[25] J.V. Goodpaster, V.L. Mcguffin, Anal. Chem. 73 (2001) 2004–2011.
[26] Y.X. Ma, H. Li, S. Peng, L.Y. Wang, Anal. Chem. 84 (2012) 8415–8421.
[27] M.L. Deng, Y.X. Ma, S. Huang, G.F. Hu, L.Y. Wang, Nano Res. 4 (2011) 685–694.
[28] J.C. Boyer, F. Vetrone, L.A. Cuccia, J.A. Capobianco, J. Am. Chem. Soc. 128 (2006) 7444–7445.
[29] M. Wang, C.C. Mi, W.X. Wang, C.H. Liu, Y.F. Wu, Z.R. Xu, C.B. Mao, S.K. Xu, ACS Nano 3 (2009) 1580–1586.
[30] R. Kumar, M. Nyk, T.Y. Ohulchanskyy, C.A. Flask, P.N. Prasad, Adv. Funct. Mater. 19 (2009) 853–859.
[31] M. Wang, W. Hou, C.C. Mi, W.X. Wang, Z.R. Xu, H.H. Teng, C.B. Mao, S.K. Xu, Anal. Chem. 81 (2009) 8783–8789.
[32] L.Y. Wang, Y.D. Li, Chem. Commun. (2006) 2557–2559.
[33] M.L. Deng, N. Tu, F. Bai, L.Y. Wang, Chem. Mat. 24 (2012) 2592–2597.
[34] L.Y. Wang, Y.D. Li, Nano Lett. 6 (2006) 1645–1649.
[35] L.Y. Wang, R.X. Yan, Z.Y. Hao, L. Wang, J.H. Zeng, H. Bao, X. Wang, Q. Peng, Y.D. Li, Angew. Chem. Int. Ed. 44 (2005) 6054–6057.
[36] G.F. Wang, Q. Peng, Y.D. Li, J. Am. Chem. Soc. 131 (2009) 14200–14201.
[37] F. Wang, X.G. Liu, J. Am. Chem. Soc. 130 (2008) 5642–5643.
[38] Y.X. Ma, H. Li, L.Y. Wang, J. Mater. Chem. 22 (2012) 18761–18767.
[39] X. Liang, X. Wang, J. Zhuang, Y.T. Chen, D.S. Wang, Y.D. Li, Adv. Funct. Mater. 16 (2006) 1805–1813.
[40] X. Wang, J. Zhuang, Q. Peng, Y.D. Li, Nature 437 (2005) 121–124.
[41] L.Y. Wang, P. Li, Y.D. Li, Adv. Mater. 19 (2007) 3304–3307.
[42] S. Huang, M. Bai, L.Y. Wang, Sci. Rep. 3 (2013) 2023, http://dx.doi.org/10.1038/srep02023.
[43] N.N. Tu, L.Y. Wang, Chem. Commun. 49 (2013) 6319–6321.
[44] H. Li, H.J. Wang, L.Y. Wang, J. Mater. Chem. C 1 (2013) 1105–1110.
[45] H.J. Wang, L.Y. Wang, Inorg. Chem. 52 (2013) 2439–2445.
[46] H. Li, L.Y. Wang, Analyst 138 (2013) 1589–1595.
[47] Y.Y. Zhu, Y.Y. Zhao, Y.X. Ma, M.L. Deng, L.Y. Wang, Luminescence 27 (2012) 74–79.
[48] Y.Y. Zhao, Y.X. Ma, H. Li, L.Y. Wang, Anal. Chem. 84 (2012) 386–395.